Structural and electrical studies of thermally annealed tungsten nitride thin film

Sharmistha Anwar, Shahid Anwar*

CSIR-Institute of Minerals and Materials Technology, Bhubaneswar Odisha, 751013, India

*Corresponding author, Tel: (+91)674-2379149; E-mail: shahidanwr@gmail.com

Received: 29 March 2016, Revised: 25 September 2016 and Accepted: 19 April 2017

DOI: 10.5185/amp.2017/603
www.vbripress.com/amp

Abstract

Present work is focused on various properties of thermally annealed tungsten nitride (WN) film. Tungsten nitride thin films on silicon (100) substrates were deposited via reactive magnetron sputtering technique. Initially Ar/N_2 flow ratio was optimized by varying N_2 gas flow between 5 to 25 sccm. 20:5 ($Ar:N_2$) was found to be the best for W_2N phase formation. Using optimized condition, a set of WN deposited and then annealed at different temperatures i.e. 200°C, 400°C and 600°C for two hours each. Various characterizations have been done using X-ray diffraction, four probe resistivity and nano-indentation test. XRD results suggest formation of pure W_2N crystalline phase of the films with face centered cubic structure. The resistivity result shows the decrease of resistivity value with increase in annealing temperature. Nano-indentation results showed hardness and elastic modulus values at 5mn load does not vary much with annealing at different temperatures. Structural, mechanical and electrical studies showed that the samples were stable up to 600°C. Thus, tungsten nitride thin films will contribute as a material suitable for long time exposure at elevated temperature for application of cutting tools.

Keywords: Annealing studies, hard coating, sputtering, nitrides, thin film technology.

Introduction

Hard coatings have been already proven to be an excellent solution to improve the wear resistance of mechanical components **[1-4]**. Transition metal nitrides based hard coatings have attracted attention because of their excellent mechanical, optical and electrical properties and interaction efficiency with light elements like nitrogen, carbon, boron and oxygen. The best known member of the group is titanium nitride **[1]**. However, its tribological properties were reduced significantly when exposed to elevated temperature, due to rapid degradation **[2]**. It has been reported that oxidation of nitride coatings is the principal mechanism leading to degradation of mechanical properties, catalytic activity and performance at elevated temperature **[3]**. The applications of these nitride coatings also require good oxidation resistance and thermal stability at elevated temperatures. Compared to the other transition metal nitrides, tungsten nitride (WN) has the lowest electrical resistivity (single crystal). Copper forms no known compounds with tungsten nitride, indicating its stability as a barrier. WN can also be deposited in amorphous form, which means that it has no grain boundaries and no fast diffusion pathways for copper. Tungsten nitride coatings also exhibiting hardness higher than 40GPa are potential candidates for protective coatings as hard coatings.

Various phases and structures of tungsten nitride compound have been reported in the literature. Cubic W_2N, hexagonal and tetragonal WN, rhombohedral WN_2 due to different nitrogen content in it **[3-5]**. Among all the phases, W_2N phase is formed as the most equilibrium phase with favorable thermodynamic conditions. In the equilibrium structure of W_2N, all the N_2 atoms are resided in the octahedral interstitial sites **[6]**. Magnetron sputtering is a useful technique for deposition of both insulators and conductors. It potentially reduces the process steps during fabrication and is also an environmentally benign process as the only gas used (for generation of plasma) is inert gas **[7-12]**.

From the literature surveys, it has been also observed that good quality tungsten nitride thin films require optimization of various parameters like nitrogen partial pressure, substrate temperature, etc. which play vital roles. The stability of films at higher temperature is a major issue and this hinders its usage in real extreme working condition. Therefore, in this current study, reactively RF magnetron-sputtered tungsten nitride thin films are synthesized and characterized under different annealing temperatures for constant time. Structural characterization, mechanical properties have been done and the results have been analyzed.

Experimental

WN thin films were deposited on Si (100) substrates using RF magnetron sputtering: Minilab Deposition System, Model ES60A, Moorfield, in ultra-high vacuum. The substrates were cleaned with soap solution to remove the greasy contaminants from the surface, and then ultrasonicated by methanol followed by distilled water for 10 minutes each. 2 Inch readymade target of tungsten (Vin Karola, USA with 99.9% purity) were used for sputtering with nitrogen as a reactive gas. In order to optimize the nitrogen ratio, the flow rate was varied as 5, 10, 15, 20 and 25 sccm, with constant argon flow rate of 20 sccm at 110W of sputtering power. During deposition, the substrate temperature was set as 150°C. The prepared samples were used for the post thermal annealing treatment at 200°C, 400°C and 600ºC for two hours under high vacuum condition of 10^{-6} mbar was achieved before annealing and 10^{-4} mbar was reached during annealing.

The crystallographic phases and structures of as-prepared and heat treated WN films were characterized by Glancing Incident X-Ray Diffraction (GIXRD), ULTIMA IV, Rigaku-Japan. The thickness of the samples was determined by Stylus Profilometer (Nanomap, AEP Technology USA). The thickness of the samples deposited is ~435 nm. The hardness and the elastic moduli of the samples were measured by UMIS Nano-indentation system, Frisher Cripps, Australia which was employed with a Berkovich diamond indenter with face angle 65.3°, and of tip radius 150 nm. Each sample was tested at 10 points, 15 micrometers apart at 5mn load for which the average value was taken as the resultant magnitude. Electrical resistivity of the sample was measured by using four-point probe technique (ZEM-3, ULVAC-RIKO Japan).

Results and discussion

X-Ray diffraction studies

Influence of Ar:N_2 ratio in W_2N phase formation

To optimize Ar to N_2 gas ratio, for the W_2N phase formation, initially deposition with different A_2 to N_2 ratio was carried out. **Fig. 1** shows the observed XRD pattern of WN thin films with different Ar/N_2 ratios, i.e. 20:5, 20:10, 20:15, 20:20, and 20:25. The XRD pattern of 20:5 (Ar:N_2) ratio among the deposited film gives well defined sharp crystalline peaks with considerable intensity and orientation. The XRD peak positions were confirm with the standard JCPDS data (25-1257, 75-0988) and were indexed as (111), (200), (220) and (311) orientation of pure W_2N face center cubic (fcc) structure **[13]**. Here we observe that with increasing Ar/N_2 ratio from 20:5 onward, peak intensities of XRD decrease gradually up to 20:10 and above that i.e. 20:15 onward, peaks disappear completely, showing the absence of crystalline W_2N phase. This may be due to the decreased growth rate with excessive N_2 gas available for reaction or amorphous phase formation. Hence, it can be concluded that 20:5 was the optimized Ar/N_2 gas ratio for achieving good quality W_2N film, similar method has already been reported for optimizing Ar/N_2 flow rate. For further studies in the following section the sample with 20:5 Ar:N_2 ratio was used throughout.

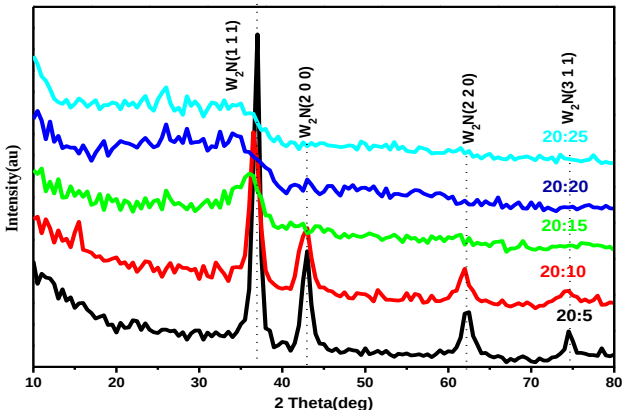

Fig. 1. GIXRD spectra of sputtered W-N films with different Ar/N_2 flow rate.

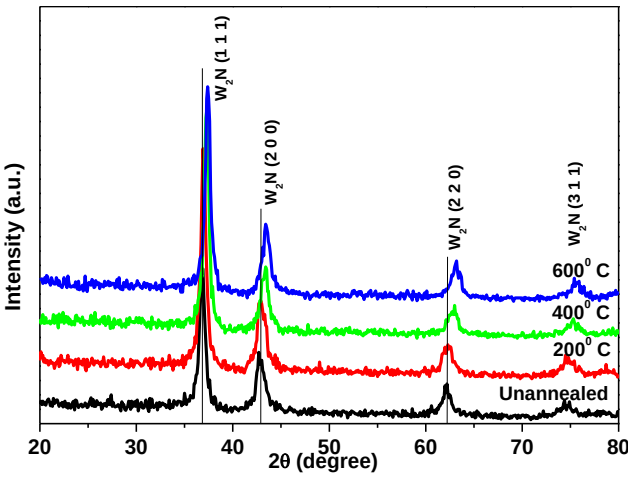

Fig. 2. GIXRD spectra of sputtered W-N films with different annealing temperature.

Influence of annealing temperatures on the prepared sample

The samples annealed at different temperatures were investigated with XRD to study its phase variation, if any. **Fig. 2** shows the XRD graph of as-prepared and annealed samples. Using XRD profile, it has been analyzed that the films posses W_2N phase with B1-NaCl type crystal structure, in which the fcc lattice sites are occupied with W atoms and half of the octahedral interstitial positions are occupied by N_2 atoms. Even after annealing from 200ºC to 600ºC temperature, single phase W_2N has been retained with only 2θ angle shift without any mix or alteration of phase. For the unannealed sample, the major peaks are shown at angle 2θ equals to 36.82º, 42.81º, 62.18º and 74.383º. When the samples are annealed at 200ºC, 400ºC and 600ºC, the measured diffraction peaks do not change significantly, but the intensity of the peaks corresponding to all (h k l) values become sharper, exhibiting better crystallinity, a slight homogeneous

higher angle shift is also observed. The increase in intensity might be due to improve crystallite sizes with increasing annealing temperature. The shift is due to the slight decrease in d-spacing with temperature. Tungsten has low reactivity towards nitrogen, so excess of nitrogen is required to form W-N compounds. So at the time of formation of tungsten nitride, nitrogen atoms reside at the interstitial positions in excess quantity which leads to defects in the lattice. During annealing, these excess nitrogen atoms release out; making lattice shrink and distorted, due to which it reduces the d-spacing of the atomic layers **[14]**. In low temperature annnealing 200°C and 400°C annealing, the shift is not very obvious because of small change in d-spacing. But in case of 600°C annealed sample, due to high temperature, number of releasing nitrogen atoms increases significantly, affecting the lattice shrinkage and distortion.

Variation of electrical resistivity

Usually for measuring the electrical resistance of thin layers, four-point probe method is used. In this method the effect of contact points resistance and interface wires is minimized. Resistivity measurements were performed between RT (~35°C) to 310°C temperature range for the as-prepared sample and samples annealed at 200°C, 400°C and 600°C. **Fig. 3** illustrates the variation of electrical resistivity of annealed W_2N thin films as a function of increasing temperatures.

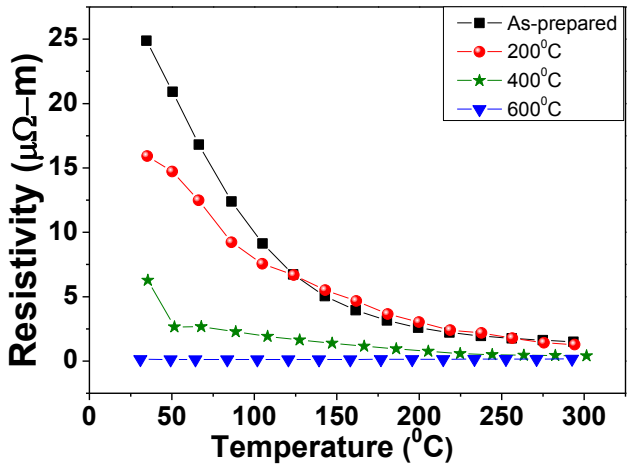

Fig. 3: Plot of resistivity with respect to change in temperature for W_2N samples annealed at various temperatures.

With an increase in annealing temperature at any temperature window, the resistivity decreases, suggesting conductivity is improving with annealing. In general, with an increase in measuring temperature for all the samples, the resistivity decreases and attains a constant minimum value at higher temperature (<250°C). Hence it can be understood, that the electrical resistivity is greatly influenced by the annealing temperature and it is inversely proportional. The highest resistivity was present for the as-deposited samples and the lowest resistivity was obtained when film highest annealed temperature (600°C). These variations in resistivity with annealing originate mainly from improved crystallinity, reduced grain boundary scattering to charge carriers, increased substitutional doping and decreased interstitial atoms as annealing temperature increased in general as reported in the literature. However, in case of nitride there is an another phenomenon that with an increase in annealing temperature from 200°C to 600°C, some nitrogen atoms may release from the lattice decreasing the resistivity of the material.

Hardness/mechanical study

In nano-indentation measurement, hardness and Young's modulus are determined as a function of displacement of the indenter from the loading-unloading curve. These are calculated from the measure of the depth or area of an indentation left by an indenter having a specific shape which is primarily elastic in nature, with a certain amount of force applied for a specific time. Hardness is defined as the resistance offered by a material to various permanent shape change or plastic deformation when a compressive force is applied. Hardness H from the nano-indentation measurement, is calculated from maximum load P_{max} divided by the actual projected contact area, A_c and can be shown as

$$H = \frac{P_{max}}{A_c}$$

In depth sensing nanoindentation, the composite modulus E* is determined from the following equation

$$E^* = \frac{\pi S}{2\beta\sqrt{A_c}}$$

where S is the meaured stiffness and β is the shape constant for Berkovich tip (β=1.034) which has been used for this indentation measurement. Young's modulus E_m is defined by the equation,

$$E_m = \left(1-\nu_m^2\right)\left(\frac{1}{E^*} - \frac{1-\nu_i^2}{E_i}\right)^{-1}$$

where υ is the Poisson's ratio, E_m is the Young's modulus of the material of experiment and E_i is the Young's modulus of indenter **[15]**.

Theoretically, tungsten nitride (W_2N) posses highest hardness as compare to that of other transition metal nitrides as it possesses the most stable equilibrium structure. But practically, during preparation of tungsten nitride, theoretically proposed ideal structure is very difficult to achieve because of the randomized selection of nitrogen atoms for interstitial positions which distort the equilibrium structure which ultimately affects the hardness **[14, 16]**. Thus the hardness of the material greatly varies according to deposition techniques and even deposition systems, so very high hardness value of

tungsten nitride has been achieved at a little percentage. In case of the samples prepared in this work, hardness and Young's modulus have been calculated by analyzing the loading-unloading curves using Oliver-Pharr method, described briefly above.

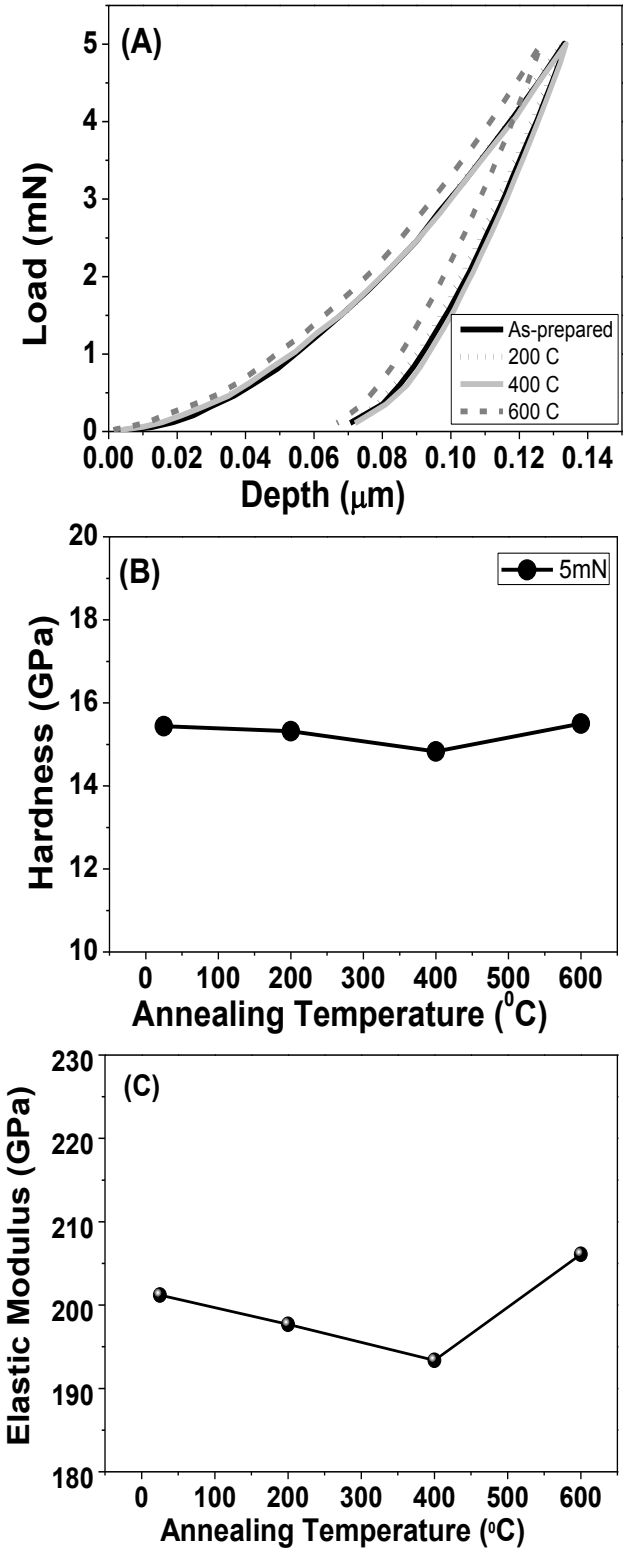

Fig. 4: (a) Loading-unloading curve (b) hardness and (c) elastic modulus of W_2N films annealed at various temperature at 5mN load.

The loading-unloading graph at 5mN of as prepared and annealed samples are shown in **Fig. 4**, which signifies the depth of indentation from which hardness and elastic modulus values have been calculated The average hardness and elastic modulus values of as prepared and annealed samples was calculated and shown in **Table 1**. The Table shows that the value of hardness and elastic modulus are almost same of as prepared and treated samples. The graphs of hardness versus annealing temperature and elastic modulus versus annealing temperature is given in **Fig. 4(b, c)**. With these graphs, it is clear that the value of hardness and elastic modulus are slightly changed up to 600°C hence these films are stable up to 600°C.

Table 1. Represent the hardness and elastic modulus values at 5mN load with respect to various annealing temperature.

Annealing Temperature (°C)	Load (5mN)	
	Hardness (H) (GPa)	Elastic Modulus (E) (GPa)
As prepared	15.44	201.1939
200	15.32	197.6986
400	14.83	193.3651
600	15.50	206.0982

Conclusion

Using reactive magnetron sputtering, we sucessfully prepared single phasic tungsten nitride thin films on silicon substrates at 110W sputtering power. Ar/N_2 gas flow ratio was optimized by varying the N_2 gas flow from 5 sccm to 25 sccm among which 20:5 ($Ar:N_2$) was found to be suitable for W_2N phase formation. The optimized films were annealed at 200°C, 400°C and 600°C for two hours each. XRD patterns of the as prepared and annealed samples showed fcc W_2N phase without any contamination present. As a result of annealing at higher temperature, XRD reflection was shifted homogeneously towards higher angles. The resistivity measurement shows the decreasing trend of resistivity with increase in measuring temperature and annealing temperature. At room temperature, the resistivity value is lower in case of annealed samples. There is slight change of hardness values with increase in annealing temperature. The highest hardness, 15.50 GPa was achieved for the sample annealed at 600°C with 5mN load. Similar pattern was observed in case of elastic modulus values. Structural, mechanical and electrical studies showed that the samples were stable up to 600°C with improved hardness and conductivity implying better quality of the films. Thus we may conclude that tungsten nitride thin films will contribute as a material suitable for long time exposure of cutting tools and diffusion barrier application at elevated temperature.

Acknowledgements

The authors would like to thank the Central Characterization Cell (CCC) at CSIR-IMMT for the characterization facility. The authors acknowledge the financial support received under 12th five-year plan project (ESC-401) of CSIR and OLP-46 of CSIR-IMMT.

References

1. Martev, I. N.; Dechev, D. A.; Ivanov, N. P.; Uzunovand, T. D.; Kashchieva, E. P.; *J. Phys.: Conf. Ser*., **2008**, *113*, 012025. **DOI:** 10.1088/1742-6596/113/1/012025
2. Polcar, T.; Cavaleiro, A.; *Int. J. Refract. Met. Hard Mater*., **2010**, *28*, 15. **DOI:** 10.1016/j.ijrmhm.2009.07.013
3. Polcar, T.; Parreira, N. M. G.; Cavaleiro, A.; *Wear*, **2008**, *265*, 319. **DOI:** 10.1016/j.wear.2007.10.011
4. Abadias, G.; Dub, S.; Shmegera, R.; *Surf. Coat. Technol*., **2006**, *200*, 6538. **DOI:** 10.1016/j.surfcoat.2005.11.053
5. Goldschidt, H. J. (Eds.); Interstitial Alloys; Plenum: USA, **1967**. **DOI:** 10.1007/978-1-4899-5880-8
6. Castanho, J.; Cavaleiro, A.; Vieira, M. T.; *Vacuum*, **1994**, *45*, 1051. **DOI:** 10.1016/0042-207X(94)90020-5
7. Asgary, S.; Hantehzadeh, M. R.; Ghoranneviss, M.; Boochani, A.; *Appl. Phys. A*, **2016**, *122*, 518. **DOI:** 10.1007/s00339-016-0045-4
8. Parreira, N. M. G.; Carvalho, N. J. M.; *Surf. Coat. Technol*., **2006**, *200*, 6511. **DOI:** 10.1016/j.surfcoat.2005.11.020
9. Kim, J. B.; Jang, B.; Lee, H. J.; Han, W. S.; Lee, D. J.; Lee, H. B. R.; Hong, T. E.; Kim, S. H.; *Mater. Lett.*, **2016**, *168*, 218. **DOI:** 10.1016/j.matlet.2016.01.071
10. Jiang, P. C.; Lai, Y. S.; Chen, J. S.; *Appl. Phys. Lett*., **2006**, *89*, 122107. **DOI:** 10.1063/1.2349313
11. Guruvenket, S.; Rao, G. M.; *Mater. Sci. Eng*., **2004**, *106*, 172. **DOI:** 10.1016/j.mseb.2003.09.016
12. Zhao, H.; Ni, F; Ye, Z.; *Surf. Eng*., **2016**, *32*, 307. **DOI:** 10.1179/1743294415Y.0000000064
13. Jiang, P.C.; Chen J. S.; Lin, Y. K.; *J. Vac. Sci. Technol., A*, **2003**, *21*, 616. **DOI:** 10.1116/1.1564029
14. Jiang, P. C.; Lai, Y. S.; Chen, J. S.; *Electrochem. Soc*., **2006**, *153*, G572. **DOI:** 10.1063/1.2349313
15. Fang, T. H.; Chang, W. J.; Lin, C. M.; *Mater. Sci. Eng. A*, **2007,** *452-453*, 715. **DOI:** 10.1016/j.msea.2006.11.008
16. Wang, S.; Yu, X.; Zhijun, L.; Zhang, R.; He, D.; Qin, J.; Zhu, J.; Han, J.; Wang, L.; Mao, H. K.; Zhang, J.; Zhao, Y.; *Chem. Mater*., **2012**, *24*, 3023. **DOI:** 10.1021/cm301516w

